IEEE Access
Multidisciplinary | Rapid Review | Open Access Journal

Received June 1, 2020, accepted June 17, 2020, date of publication June 22, 2020, date of current version July 1, 2020.

Digital Object Identifier 10.1109/ACCESS.2020.3004042

Improved Torque Ripple Minimization Technique With Enhanced Efficiency for Surface-Mounted PMSM Drives

JINUK KIM, SANG-WOOK RYU, MUHAMMAD SAAD RAFAQ, HAN HO CHOI, (Member, IEEE), AND JIN-WOO JUNG, (Member, IEEE)
Division of Electronics and Electrical Engineering, Dongguk University, Seoul 04620, South Korea

Corresponding author: Jin-Woo Jung (jinwjung@dongguk.edu)

This work was supported by the Basic Science Research Program through the National Research Foundation of Korea (NRF) funded by the Ministry of Education under Grant 2018R1D1A1B07046873.

ABSTRACT This paper proposes an improved torque ripple minimization (TRM) method using model-based loss minimization (LM) control to reduce the torque ripples and enhance the efficiency for surface-mounted permanent magnet synchronous motor (SPMSM) drives. The conventional SPMSM drives usually achieve the maximum torque per ampere (MTPA) control by applying the zero d-axis current (ZDC) and ignore an actual core loss resistance in the controller design. Unlike the conventional MTPA method, the proposed TRM selects the appropriate d-axis current value by making the derivative of the electromagnetic torque equal to zero in the SPMSM drives. Consequently, the proposed method can improve the torque ripples and efficiency compared to the conventional MTPA. Using the proportional-integral (PI) controllers, comparative experimental verifications between the proposed model-based TRM, the conventional model-based MTPA, and the conventional model-based LM are performed through a prototype SPMSM drive with a TI TMS320F28335 digital signal processor (DSP).

INDEX TERMS Core loss resistance, maximum torque per ampere (MTPA), model-based loss minimization (LM) control, surface-mounted permanent magnet synchronous motor (SPMSM), torque ripple minimization (TRM).

I. INTRODUCTION

Among various types of ac motors, the permanent magnet synchronous motors (PMSMs) are increasingly used in the industrial applications (e.g., electric vehicles (EVs), machine tools, industrial robots, home appliances, etc.) owing to their outstanding advantages such as high efficiency, compact size, low maintenance cost, high power density, high reliability, and high torque-to-inertia ratio [1]–[3]. In the surface-mounted PMSMs (SPMSMs), it is necessary to reduce the torque ripples that cause undesirable acoustic noises, torsional vibrations, and shaft failures [4]–[6]. Generally, there are two sources of the torque ripples generated in the SPMSMs: 1) distorted magnetic flux density waveforms in the air gap and 2) back-electromotive force (EMF) harmonics [4]. Other factors that influence the torque ripples are the current measurement errors and unbalanced stator phase currents [5].

Generally, the torque ripples generated in the SPMSMs can be reduced by either the machine designs or control designs [2]–[4]. First, several machine designs such as employing a fractional number of slots per pole, skewing magnets or stator lamination slots, and reshaping magnets are presented to suppress the torque ripples [2]–[5]. However, specialized machine designs increase the complexity in the production process and then result in higher machine cost [6], [7].

Next, the torque ripples can be attenuated by the control designs with maximum torque per ampere (MTPA) method (i.e., zero d-axis current (ZDC, $i_{ds} = 0$)) such as proportional-integral (PI) control [2], [8], deadbeat control [9], [10] iterative learning control (ILC) [11], [12], repetitive control [13], sliding mode control (SMC) [14], [15], and model predictive control (MPC) [7], [16]. The conventional

The associate editor coordinating the review of this manuscript and approving it for publication was Zhong Wu.

PI control has a simple structure compared to the advanced control strategies [2]. However, it is difficult to effectively suppress the torque ripples because it is vulnerable to the parameter uncertainties and external disturbances [8]. The deadbeat control can be merged with the prediction algorithm to reduce the torque ripples [9]. However, the torque ripples are reduced to a few percent and the complexity are increased due to the feedforward compensators that should be tuned for the specific motor [10]. The ILC can supply an internal model which can compensate for any periodic components in the torque [11]. However, this method has considerable torque ripples because it does not consider the dynamics of load torque [12]. In [13], the repetitive control eliminates the periodic tracking errors and torque ripples of the control loop by using some compensation control terms. However, it has the inherent problems that the controller gains should be carefully selected and the system response is slow. The SMC can deal with both the periodic torque ripples and non-periodic disturbances of the system [14]. However, it is difficult to determine the upper limit of system disturbances owing to the sliding mode chattering [15]. In recent years, the MPC is being considered as an attractive method in the SPMSM drives due to its fast dynamics at different system constraints [7]. However, the large torque and current ripples in both the steady and transient states degrade the performance of the SPMSM drives [16]. These MTPA based control methods have been presented to reduce the copper loss in the SPMSM drives and improve the drive efficiency [2], [7]–[16]. However, these methods cannot effectually reduce the iron loss because the core loss resistance is not considered in the control design for an SPMSM drive. Thus, despite the reduced copper loss, it is difficult for the MTPA method to effectively reduce the electrical losses which consist of both the copper loss and iron loss [2], [7]–[16].

To minimize the electrical losses of the SPMSMs, the loss minimization (LM) techniques are presented, which employ an appropriate nonzero d-axis current (NZDC, $i_{ds} \neq 0$) control with a core loss resistance [17]–[21]. In these techniques, as the speed increases, the d-axis stator current generally increases, which results in the increased copper loss [17], [18]. In the LM techniques [19]–[21], the search-based methods and model-based methods are mainly utilized to minimize the electrical losses. First, the former does not require the SPMSM parameters, so it is easy to implement. However, it may lose out on the dynamic performance and suffer from the toque ripples [19]. Next, the latter depends on the motor parameters, but it is widely used because of their fast dynamic response and reduced torque ripples as compared to the search-based methods [20], [21]. Moreover, few researches have been presented in the literature on minimizing the torque ripples with LM techniques, but the torque ripples are less reduced compared to the MTPA based control designs [22], [23]. Thus, using either the MTPA or LM control has a trade-off between the torque ripples and electrical losses in the SPMSM drives.

This paper proposes an improved torque ripple minimization (TRM) technique using model-based loss minimization (LM) control that can lower the torque ripples and improve the efficiency for voltage source inverter (VSI)-fed SPMSM drives. The advantages of the proposed TRM method are summarized as follows: 1) As compared to the model-based LM technique [19]–[21], the torque ripple components are significantly reduced owing to the appropriately selected d-axis current value by making the derivative of the electromagnetic torque equal to zero in the SPMSM drives. 2) Even if the d-axis stator current increases the copper loss of the SPMSM, the proposed TRM control approach with a core loss resistance minimizes the electrical losses by achieving the smaller iron loss compared to the conventional MTPA. The comparative experimental studies on a prototype VSI-fed SPMSM drive with a TI TMS320F28335 digital signal processor (DSP) are performed to check the improved torque ripples and efficiency between the proposed model-based TRM, the conventional model-based MTPA, and the conventional model-based LM.

II. TRM CONTROL DESIGN USING MODEL-BASED LM WITH A CORE LOSS RESISTANCE FOR SPMSM DRIVES

This section presents an improved TRM method using model-based LM with a core loss resistance (CLR) for SPMSM drives to decrease the torque ripples and enhance the efficiency as compared with the conventional MTPA with ZDC (i.e., $i_{ds} = 0$) without a CLR [4]–[6].

A. DYNAMIC MODEL FOR SPMSM DRIVES

The conventional dynamic model of the SPMSM in the rotating d-q reference frame [1]–[3] can be described as

$$\begin{cases} \dot{\omega} = k_1 i_{qs} - k_2 \omega - k_3 T_L \\ \dot{i}_{qs} = -k_4 i_{qs} - k_5 \omega + k_6 v_{qs} - \omega i_{ds} \\ \dot{i}_{ds} = -k_4 i_{ds} + k_6 v_{ds} + \omega i_{qs} \\ \lambda_s = \sqrt{\lambda_d^2 + \lambda_q^2} \end{cases} \tag{1}$$

where

$$k_1 = \frac{3}{2}\frac{1}{J}\frac{p^2}{4}\lambda_m, \quad k_2 = \frac{B}{J}, \; k_3 = \frac{p}{2J}, \; k_4 = \frac{R_s}{L_s}, \; k_5 = \frac{\lambda_m}{L_s}, \quad k_6 = \frac{1}{L_s},$$

ω is the rotor speed, i_{ds} and i_{qs} are the stator currents in the d-q frame, T_L is the load torque, v_{ds} and v_{qs} are the stator voltages in the d-q frame (i.e., control inputs), L_s and R_s are the stator inductance and resistance, p is the number of poles, J is the moment of inertia, B is the coefficient of viscous friction, λ_m is the magnet flux linkage, λ_s is the stator flux linkage, and λ_d ($=L_s i_{ds} + \lambda_m$) and λ_q ($=L_s i_{qs}$) are the stator flux linkages in the d-q frame, respectively. Fig. 1 shows the conventional equivalent circuit model for SPMSM drives in the rotor reference frame.

The electrical losses (P_T) of SPMSMs, which consist of the copper loss (P_{Cu}) and iron loss (P_{Fe}), can be approximately

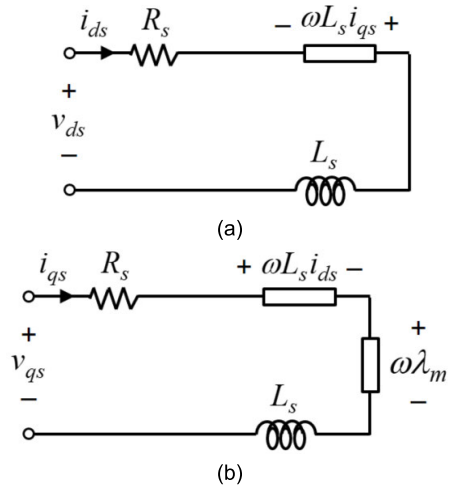

FIGURE 1. The conventional equivalent circuit model for SPMSM drives in the rotor reference frame. (a) *d*-axis. (b) *q*-axis.

calculated as [17], [18]

$$P_T = P_{Cu} + P_{Fe} = R_s(i_{ds}^2 + i_{qs}^2) + P_{Hy} + P_{Eddy} \tag{2}$$

where $P_{Cu} = R_s(i_{ds}^2 + i_{qs}^2)$, $P_{Fe} = P_{Hy} + P_{Eddy}$, P_{Hy} is the hysteresis loss, and P_{Eddy} is the eddy current loss. Also, the P_{Hy} and P_{Eddy} of the iron loss (P_{Fe}) are determined by the flux density (B) and rotor speed (ω) as

$$\begin{aligned} P_{Fe} &= P_{Hy} + P_{Eddy} = k_{Hy}B^{\beta}\omega + k_{Eddy}B^2\omega^2 \\ &\approx k_{Fe}B^2\omega^{\gamma} \end{aligned} \tag{3}$$

where $P_{Hy} = k_{Hy}B^{\beta}\omega$, $P_{Eddy} = k_{Eddy}B^2\omega^2$, k_{Hy}, k_{Eddy}, and k_{Fe} are constants, β is in the range of 1.8∼2.2, and γ is in the range of 1.5∼1.6 [19]–[21]. Based on the dynamic model (1), the iron loss (3) can be expressed by the stator flux linkage (λ_s) as

$$\begin{aligned} P_{Fe} &= C_{Fe}\omega^{\gamma}\lambda_s^2 = C_{Fe}\omega^{\gamma}\left(\lambda_d^2 + \lambda_q^2\right) \\ &= C_{Fe}\omega^{\gamma}\left((L_s i_{ds} + \lambda_m)^2 + L_s^2 i_{qs}^2\right) \end{aligned} \tag{4}$$

where C_{Fe} is the iron loss coefficient.

As clearly presented in (4), it is difficult for the MTPA method with ZDC (i.e., $i_{ds} = 0$) to effectively minimize the electrical losses despite the reduced copper loss because the d-axis stator flux linkage (λ_d), which affects the iron loss (P_{Fe}), cannot be controlled with this method [19]–[21].

B. IMPROVED TRM METHOD USING MODEL-BASED LM

In the SPMSM drives, the torque ripples and electrical losses should be minimized simultaneously to improve the dynamic performance [4]–[6] and motor efficiency [19]–[21]. Generally, the conventional MTPA method is employed to reduce the torque ripples and minimize the copper loss by utilizing the ZDC (i.e., $i_{ds} = 0$). However, the iron loss (P_{Fe}) cannot be minimized because of no control on the d-axis stator flux linkage (λ_d) [19]–[21]. On the other hand, the model-based LM method with a core loss resistance minimizes the electrical losses by choosing the appropriate d-axis demagnetizing current (i_{od}) and reducing the iron loss (P_{Fe}). However, the conventional LM method cannot effectively reduce the torque ripples in the SPMSM drives [22], [23]. Thus, this paper presents an enhanced TRM method using the model-based LM with a core loss resistance to reduce both the torque ripples and electrical losses of the SPMSM drives. Fig. 2 shows the equivalent circuit model with a simplified R_c for SPMSM drives where i_{cd} ($=i_{ds} - i_{od}$) and i_{cq} ($=i_{qs} - i_{oq}$) are the core loss currents in the d-q frame, i_{od} and i_{oq} are the d-axis demagnetizing current and q-axis torque-generating current, respectively, and v_{od} and v_{oq} are the core loss voltages in the d-q frame.

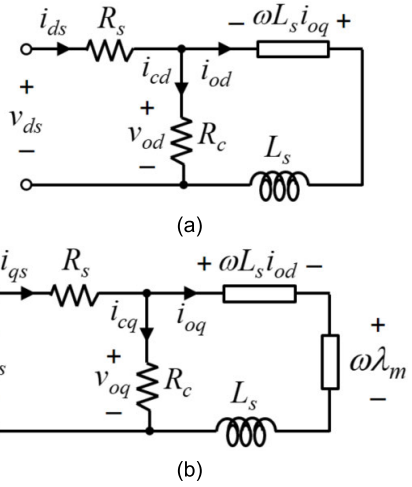

FIGURE 2. The equivalent circuit model with a simplified core loss resistance for SPMSM drives in the rotor reference frame. (a) *d*-axis. (b) *q*-axis.

From the equivalent circuit model with a simplified core loss resistance (CLR) shown in Fig. 2, the dynamic model (1) can be modified as the following [19]–[21]:

$$\begin{cases} \dot{\omega} = k_1 i_{oq} - k_2\omega - k_3 T_L \\ \dot{i}_{oq} = -k_4 i_{oq} - \eta k_5\omega + k_6 v_{qs} - \eta\omega i_{od} \\ \dot{i}_{od} = -k_4 i_{od} + k_6 v_{ds} + \eta\omega i_{oq} \\ \lambda_s = \sqrt{\lambda_{od}^2 + \lambda_{oq}^2} \end{cases} \tag{5}$$

where λ_{od} ($=L_s i_{od} + \lambda_m$) and λ_{oq} ($=L_s i_{oq}$) are the stator flux linkages in the d-q frame, η ($=1 + R_s/R_c$) is the resistance ratio, and R_c is the CLR.

From the dynamic model (5) of the SPMSM with a CLR, the electromagnetic torque (T_e) is given by

$$T_e = \frac{3}{2}\frac{p}{2}\left(\lambda_m i_{oq} + \left(L_{qs} - L_{ds}\right) i_{od} i_{oq}\right) = \frac{3}{2}\frac{p}{2}\lambda_m i_{oq} = \frac{k_1}{k_3} i_{oq} \tag{6}$$

where it is considered as the $L_{ds} = L_{qs} = L_s$ for the SPMSM.

It is noted that the minimum torque ripples are achieved by differentiating the T_e in (6) and then setting it to zero

as $dT_e/dt = 0$. Thus, the time derivative of the electromagnetic torque (i.e., torque ripple components, dT_e/dt) can be expressed as follows:

$$\frac{dT_e}{dt} = \frac{k_1}{k_3}\dot{i}_{oq} = \frac{k_1}{k_3}\left(-k_4 i_{oq} - \eta k_5 \omega + k_6 v_{qs} - \eta \omega i_{od}\right). \quad (7)$$

The above equation (7) implies that the torque ripples can be minimized (i.e., $dT_e/dt = 0$) by using the following d-axis demagnetizing current reference (i_{odr}):

$$i_{odr} = -k_5 - \frac{k_4 i_{oq}}{\eta\omega} + \frac{k_6 v_{qs}}{\eta\omega}. \quad (8)$$

Considering the stator voltage and current constraints [22], the proposed TRM (8) can be rewritten as

$$i_{odr} = \begin{cases} 0 & if\ i_{ds} \geq 0 \\ i_{odr}\ in\ (8) & if\ -\sqrt{I_{s\max}^2 - i_{qs}^2} \leq i_{ds} < 0 \\ -\sqrt{I_{s\max}^2 - i_{qs}^2} & otherwise \end{cases} \quad (9)$$

where I_{smax} ($\geq\sqrt{(i_{ds}^2 + i_{qs}^2)}$) is the maximum stator current determined by the rated current of the machine and inverter.

From the first-order derivative of the T_e (7), the second-order derivative of the T_e is given by

$$\begin{aligned} \frac{d^2T_e}{dt^2} &= \frac{d}{dt}\left(\frac{k_1}{k_3}\dot{i}_{oq}\right) \\ &= -\frac{k_1 k_4}{k_3}\dot{i}_{oq} - \frac{\eta k_1 k_5}{k_3}\dot{\omega} - \frac{\eta k_1}{k_3}\frac{d}{dt}(\omega i_{od}) \end{aligned} \quad (10)$$

where the first-order derivative of the v_{qs} is zero (i.e., $\dot{v}_{qs} = 0$). From the dynamic model (5) of the SPMSM, it can be rewritten as

$$\begin{aligned} \frac{d^2T_e}{dt^2} &= \underbrace{-\frac{k_1 k_4}{k_3}\left(-k_4 i_{oq} - \eta k_5 \omega + k_6 v_{qs} - \eta \omega i_{od}\right)}_{dTe/dt} \\ &\quad - \frac{\eta k_1 k_5}{k_3}\left(k_1 i_{oq} - k_2\omega - k_3 T_L\right) \\ &\quad - \frac{\eta k_1}{k_3}\left(\begin{matrix}\left(k_1 i_{oq} - k_2\omega - k_3 T_L\right) i_{od} \\ +\omega\left(-k_4 i_{od} + k_6 v_{ds} + \eta\omega i_{oq}\right)\end{matrix}\right). \end{aligned} \quad (11)$$

Since $dT_e/dt = 0$ based on (7), it can be rewritten as

$$\begin{aligned} \frac{d^2T_e}{dt^2} &= \underbrace{-\frac{\eta k_1 k_5}{k_3}\left(k_1 i_{oq} - k_2\omega - k_3 T_L\right)}_{Term\ 1} \\ &\quad \underbrace{-\frac{\eta k_1 i_{od}}{k_3}\left(k_1 i_{oq} - k_2\omega - k_3 T_L\right)}_{Term\ 2} \\ &\quad \underbrace{-\frac{\eta k_1 \omega}{k_3}\left(-k_4 i_{od} + k_6 v_{ds} + \eta\omega i_{oq}\right)}_{Term\ 3}. \end{aligned} \quad (12)$$

Based on the nominal parameters of the SPMSM, *Term 3* is positive and the most dominant one in (12) as compared to *Terms 1* and *2*, where $v_{ds} = (k_4 i_{od} - \eta\omega i_{oq})/k_6 < 0$ in *Term 3*. Thus, it can be inferred that the second-order derivative of the T_e is greater than zero (i.e., $d^2T_e/dt^2 > 0$) which proves that the minimum value of electromagnetic torque ripples can be achieved at $dT_e/dt = 0$.

Thus, the torque ripple components (i.e., dT_e/dt (7)) are significantly reduced owing to the proposed TRM law (8) and voltage and current constraints (9). Note that the torque ripple factor (TRF) is presented to evaluate the effectiveness for torque ripple minimization as [24]

$$TRF\ (\%) = \frac{T_{pk-pk}}{T_{rated}} \times 100 \quad (13)$$

where T_{pk-pk} is the peak-to-peak torque ripple and T_{rated} is the rated torque.

Remark 1: Based on the dynamic model (5) and Fig. 2, the iron loss (4) can be expressed by the core loss resistance and core loss currents in the following [17]–[20]:

$$\begin{aligned} P_{Fe} &= \frac{v_{od}^2 + v_{oq}^2}{R_c} = \frac{\omega^2}{R_c}\left(\left(L_s i_{oq}\right)^2 + \left(\lambda_m + L_s i_{od}\right)^2\right) \\ &= \frac{\omega^2}{R_c}\left(\lambda_{oq}^2 + \lambda_{od}^2\right) = R_c\left(i_{cd}^2 + i_{cq}^2\right) \end{aligned} \quad (14)$$

where $i_{cd} = -\omega L_s i_{oq}/R_c$ and $i_{cq} = (\omega\lambda_m + \omega L_s i_{od})/R_c$. It is noted that the average voltage across the stator inductance (L_s) is zero in the steady-state [19]–[21]. It can be seen from (14) that the iron loss (P_{Fe}) can be reduced with the negative d-axis demagnetizing current (i_{od}). Thus, the value of the d-axis stator current (i_{ds} ($=i_{od} + i_{cd}$)) is also negative. Based on the dynamic model (1), the injection of the negative i_{ds} affects the air-gap field and the v_{qs} which includes the back-EMF (i.e., $\omega\lambda_m$), so it can change the speed of an interior PMSM (IPMSM) that operates in the constant power region [25]. However, for the SPMSM, the T_e is not affected because it only works in the constant torque region (i.e., below the rated speed (ω_{rated})) and is determined by the magnetic flux (λ_m) and q-axis current (i_{qs}) as shown in (6). Fig. 3 shows the voltage and current limit boundaries of the conventional MTPA and the proposed TRM for an SPMSM drive where the voltage limit boundary is centered at $(-\lambda_m/L_s, 0)$. As shown in Fig. 3, the voltage limit ellipse decreases due to the proposed TRM (8) below the ω_{rated} (i.e., constant torque region). However, it is still large enough

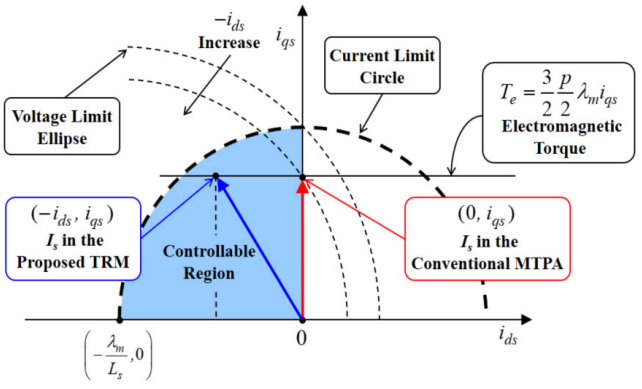

FIGURE 3. Voltage and current limit boundaries of the conventional MTPA and the proposed TRM for an SPMSM drive.

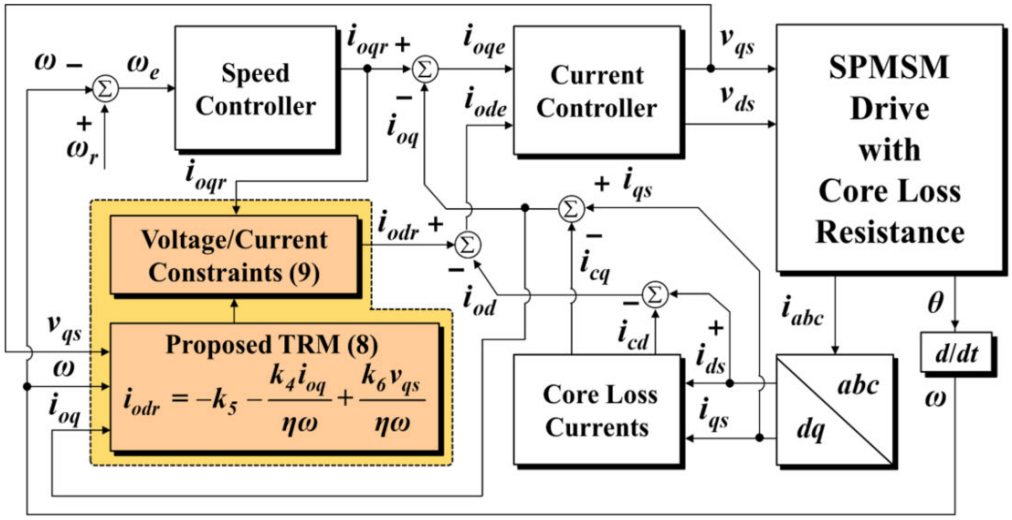

FIGURE 4. Block diagram of the proposed TRM with a core loss resistance for an SPMSM drive.

to encompass the current limit circle, so the T_e in (6) is not affected due to the constant value of i_{qs}.

Consequently, the proposed TRM law (8) can improve at once the torque ripples and efficiency compared to the conventional MTPA method with ZDC (i.e., $i_{ds} = 0$) without a core loss resistance [2].

Remark 2: In the conventional model-based LM method [20] that can minimize the electrical loss (P_T), the d-axis demagnetizing current reference (i_{odr}^{LM}) in (15) is obtained by differentiating the P_T with respect to i_{od} and then putting the derivative to zero (i.e., $dP_T/di_{od} = 0$). Thus, the i_{odr}^{LM} can be expressed by the resistance ratio (η) as

$$\begin{aligned} i_{odr}^{LM} &= -\frac{\omega^2 L_s \lambda_m (R_s + R_c)}{R_s R_c^2 + \omega^2 L_s^2 (R_s + R_c)} \\ &= -k_5 + \frac{k_4 k_5 k_6 R_c}{k_4 k_6 R_c + \eta\omega^2}. \end{aligned} \tag{15}$$

Based on the conventional LM method (15) and the proposed TRM method (8), it can be seen that the values of i_{odr} in both methods are different in the low and medium-speed regions because they are determined by several parameters such as the L_s, R_s, and λ_m as compared to the rotor speed (ω). Contrarily, it can be noted that in the high-speed region (i.e., above about 80% of rated speed), the value of i_{odr} in the proposed TRM method (8) is almost the same as the value of i_{odr}^{LM} in the conventional model-based LM method (15). It means that the speed ω exists in a denominator of i_{odr} in both methods, so it can be ignored at the high speed and then only $-k_5$ ($=-\lambda_m/L_s$) remains as follows:

$$i_{odr}^{LM} = -k_5 + \frac{k_4 k_5 k_6 R_c}{k_4 k_6 R_c + \eta\omega^2} \approx -k_5, \quad if \ |\omega| \gg 1, \tag{16a}$$

$$i_{odr} = -k_5 - \frac{k_4 i_{oq}}{\eta\omega} + \frac{k_6 v_{qs}}{\eta\omega} \approx -k_5, \quad if \ |\omega| \gg 1. \tag{16b}$$

Thus, the proposed TRM law (16b) can also reduce the iron loss (P_{Fe}) as the i_{odr}^{LM} (16a) in the high-speed region (i.e., above rated speed). It means that the proposed TRM law (8) can reduce the electrical losses (P_T) in the high-speed region, similar to the conventional model-based LM method [20] as presented in (16a). Fig. 4 shows the block diagram of the proposed TRM with a core loss resistance (CLR) for an SPMSM drive using the conventional speed and current controllers where ω_r is the speed reference and i_{ode} and i_{oqe} are the input errors of the current controller in the d-q frame, respectively. In case of the conventional MTPA method without a CLR, the i_{oq} and i_{od} are equal to the i_{qs} and i_{ds}, respectively because the value of the R_c is infinite (i.e., $i_{cd} = i_{cq} = 0$). Note that the proposed TRM can be applied to various types of controllers (e.g., PI controller, linear quadratic regulator (LQR), fuzzy controller, etc.) that are likely to decrease the torque ripples and improve the efficiency.

In this paper, the design procedure for the proposed model-based TRM (9) is summarized as follows:

Step 1) Build the dynamic model of the SPMSM with a core loss resistance (5) in the synchronously rotating d-q frame.

Step 2) Select the d-axis demagnetizing current reference (i_{odr}) (8) by differentiating the P_T with respect to i_{od} and then putting the derivative to zero as $dP_T/di_{od} = 0$.

Step 3) Select the i_{odr} by considering the stator voltage and current constraints in (9). Since the i_{odr} in (9) should exist within the value of the I_{smax} to obtain the optimum value of the d-axis current and maintain the high-torque capability in the SPMSM drives [2]. Thus, if the i_{odr} exists within the voltage and current constraints, then quit, or else, return to the start of *Step 3*.

Step 4) Get the control input (v_{ds} and v_{qs}) by taking the i_{ode} and i_{oqe} as the inputs to the current controller.

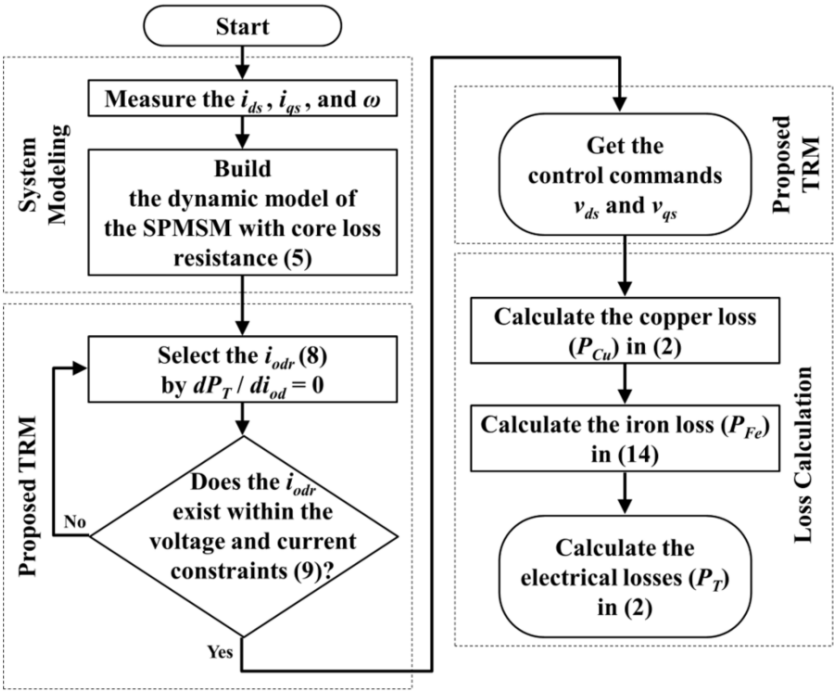

FIGURE 5. Flowchart of the proposed model-based TRM for an SPMSM drive.

Step 5) Calculate the electrical losses (P_T) which consist of the copper loss (P_{Cu}) in (2) and iron loss (P_{Fe}) in (14).

For an easy understanding, Fig. 5 illustrates the flowchart of the proposed model-based TRM with a core loss resistance for an SPMSM drive using the conventional speed and current controllers.

III. COMPARATIVE EXPERIMENTAL RESULTS AND VERIFICATIONS

To demonstrate the efficacy of the proposed TRM law, three control methods (i.e., the proposed model-based TRM, conventional model-based MTPA [2], and conventional model-based LM [20]) are comparatively investigated with the conventional PI speed and current controllers in a cascaded control structure that have been widely used in the industry owing to its simplicity and satisfactory performance [2], [8].

A. HARDWARE PLATFORM

Fig. 6 exhibits the overall schematic diagram and experimental prototype with a DSP-based VSI-fed SPMSM drive. The nominal parameters of an SPMSM experimental platform in Table 1 are measured by the LCR meter (LCR-819) and provided by the KOMOTEK CO., LTD. (KANZ series servo motor specifications). As shown in Fig. 6, an incremental encoder (E40H6-2500) is installed to obtain the rotor position (θ) and speed (ω) of an SPMSM drive and two stator phase currents (i_a, i_b) are measured by Hall effect sensors (ACS712T).

TABLE 1. Nominal parameters of a prototype SPMSM drive.

System Parameters	Descriptions	Values
Switching Frequency	f_{sw}	5 [kHz]
Sampling Time	T_s	200 [μs]
Rated Power	P_{rated}	750 [W]
Rated Torque	T_{rated}	2.4 [N·m]
Rated Speed	ω_{rated}	3000 [r/min]
Rated Phase-to-Phase Voltage	V_{rated}	220 [V]
Rated Phase Current	I_{rated}	4.3 [A]
Stator Inductance	L_s	3.2 [mH]
Stator Resistance	R_s	0.43 [Ω]
Magnetic Flux Linkage	λ_m	0.085 [V·s/rad]
Equivalent Rotor Inertia	J	0.002 [kg·m^2]
Number of Poles	p	8
Viscous Friction Coefficient	B	0.0002 [N·m·s/rad]

Next, the stator currents (i_{ds}, i_{qs}) in the d-q frame can be obtained from the measured two stator phase currents (i_a, i_b) via *Park's* and *Clarke's* transformations. In this paper, the command signals (v_{ds}, v_{qs}) from the PI current controller are generated by the space vector pulse width modulation (SVPWM) algorithm in real-time and then sent to the three-phase inverter through a TI TMS320F28335 DSP board. Also, the switching frequency (f_{sw}) and sampling time (T_s) are selected as 5 kHz and 200 μs, respectively. Note that the core loss resistance (i.e., R_c) is directly obtained with the above specifications of the SPMSM [19]–[21] as

$$R_c = \frac{\omega^2 \left(\lambda_d^2 + \lambda_q^2\right)}{P_{si} - P_{out}} = 129.06\,[\Omega] \tag{17}$$

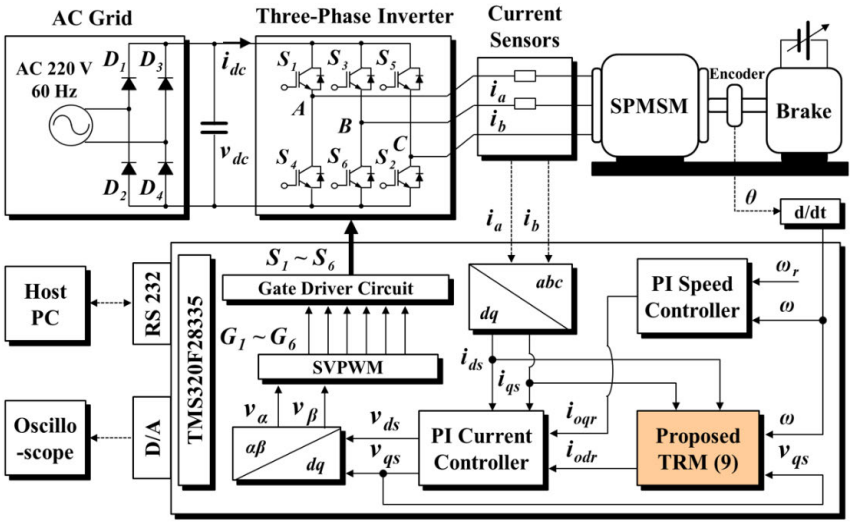

(a)

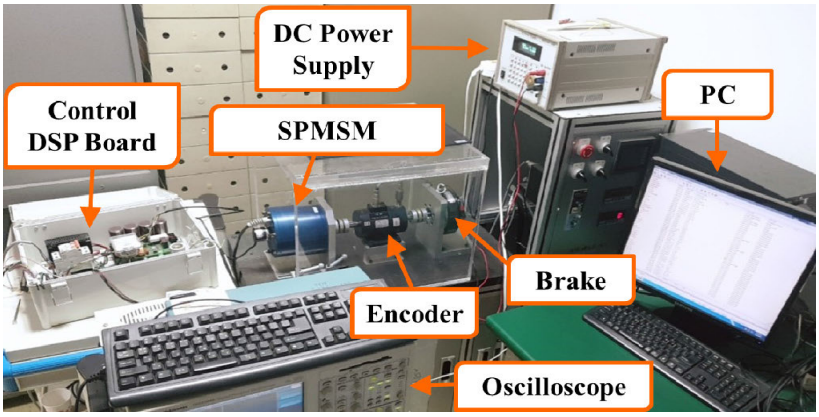

(b)

FIGURE 6. Experimental platform with a DSP-based VSI-fed SPMSM drive. (a) Overall schematic diagram. (b) Experimental prototype.

where P_{si} and P_{out} are the semi-input power and output power, respectively. Based on (14) and (17), the electrical losses (P_T) which consist of the copper loss (P_{Cu}) in (2) and iron loss (P_{Fe}) in (14) can be estimated.

The comparative experiments of the three control methods are performed with the conventional PI speed and current controllers under the following two cases:

Case 1: Speed step-change (i.e., ω_r: $-600 \rightarrow 1200 \rightarrow 3000$ r/min) under T_L set at 2.4 N · m.

Case 2: Load torque step-change (i.e., T_L: $0.48 \rightarrow 1.44 \rightarrow 2.4$ N · m) under ω_r set at 3000 r/min.

According to the commonly used PI tuning rules [2], [8], the PI current controller bandwidth ω_{cc} ($\omega_{cc} = 2\pi \cdot 200$ rad/s; $f_{cc} = 200$ Hz) is chosen as 1/25 of the f_s (=5 kHz), whereas the PI speed controller bandwidth ω_{sc} ($\omega_{sc} = 2\pi \cdot 25$ rad/s; $f_{sc} = 25$ Hz) is selected as 1/8 of the ω_{cc}.

B. TORQUE RIPPLE MINIMIZATION INVESTIGATION

Fig. 7 demonstrates the comparative experimental results of the three control methods under *Case 1*. As the speed reference (ω_r) suddenly changes (i.e., ω_r: $-600 \rightarrow 1200 \rightarrow 3000$ r/min), the significant torque ripples can be found in the conventional MTPA (i.e., 1.06/1.02/1.02 N · m, respectively) and the conventional model-based LM (i.e., 1.17/1.18/1.14 N · m, respectively) during the steady-state at each speed as shown in Fig. 7(a)–(b). Meanwhile, Fig. 7(c) shows a remarkable reduction in torque ripples by using the proposed TRM (i.e., 0.77/0.76/0.71 N · m, respectively). In Fig. 7, the q-axis stator currents (i_{qs}) of the three different control methods remain at 5.1 A during the steady-state corresponding to the load torque of 2.4 N · m. Moreover, it can be seen in Fig. 7(a) that the i_{ds} of the conventional MTPA is almost zero, while the i_{ds} values of the conventional LM and the proposed TRM in Fig. 7(b)–(c) are observed as $-1.20/-1.32/-2.51$ A and $-0.3/-2.1/-2.82$ A during the steady-state, respectively.

Fig. 8 shows the comparative experimental results of the three control methods under *Case 2*. As the T_L abruptly varies (i.e., T_L: $0.48 \rightarrow 1.44 \rightarrow 2.4$ N · m), the conventional MTPA (i.e., 0.94/0.98/0.96 N · m, respectively) and the conventional

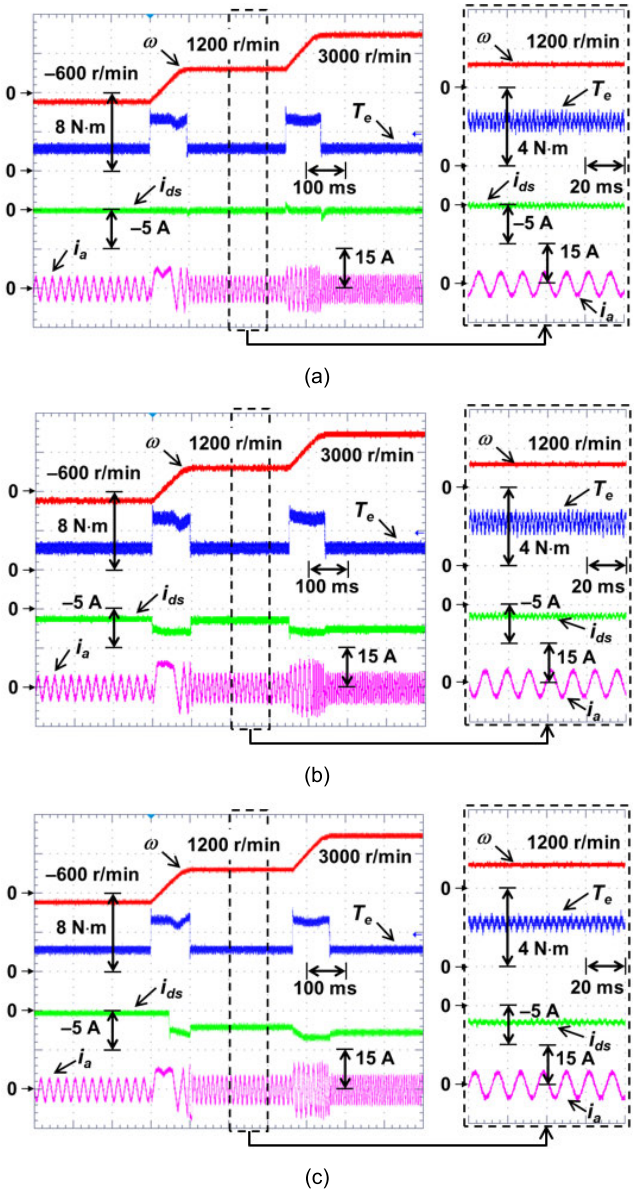

FIGURE 7. Comparative experimental results under *Case 1*. (a) Conventional model-based MTPA. (b) Conventional model-based LM. (c) Proposed model-based TRM.

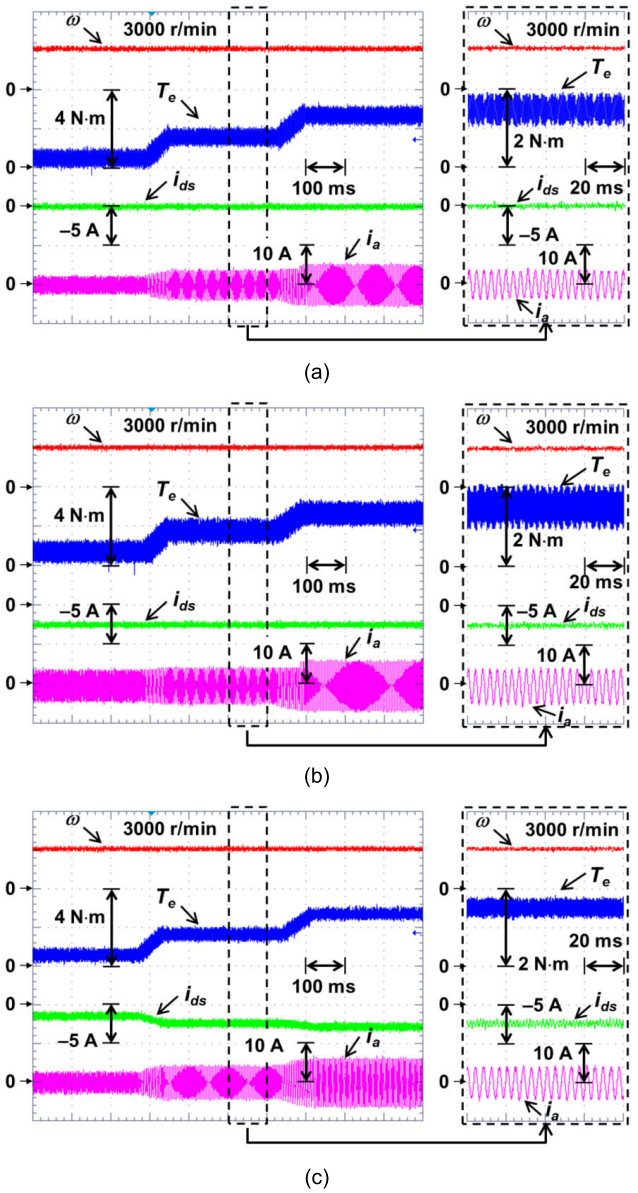

FIGURE 8. Comparative experimental results under *Case 2*. (a) Conventional model-based MTPA. (b) Conventional model-based LM. (c) Proposed model-based TRM.

model-based LM (i.e., 1.10/1.12/1.08 N · m, respectively) shown in Fig. 8(a)–(b) have some significant torque ripples in the steady-state, respectively. Meanwhile, the proposed TRM during the steady-state in Fig. 8(c) shows the comparatively reduced torque ripples of 0.72/0.69/0.63 N · m, respectively. With the increase in the T_L, the values of the i_{qs} in the three different control methods also rise as 1.72/3.63/5.1 A, respectively. In Fig. 8(a)–(b), the i_{ds} in the conventional MTPA (0 A) and the conventional LM (–2.52 A) are almost constant. However, Fig. 8(c) highlights that the i_{ds} of the proposed TRM increases (i.e., –1.56/–2.53/–2.81 A, respectively) as the T_L increases to utilize the optimal values of the i_{ds}.

C. ELECTRICAL LOSSES INVESTIGATION

Fig. 9 indicates the electrical losses ($P_T = P_{Cu} + P_{Fe}$) of the three control methods under *Case 1*. As the speed reference (ω_r) increases (i.e., ω_r: $-600 \rightarrow 1200 \rightarrow 1800 \rightarrow 2400 \rightarrow 3000$ r/min), it can be shown from Fig. 9 that the P_T increases. In Fig. 9(a), the conventional model-based MTPA has the lower copper loss (P_{Cu}) (i.e., 11.14/11.18/11.32/11.45/11.45 W, respectively) because it minimizes the stator current by achieving the MTPA without considering the core loss resistance. Meanwhile, the iron loss (P_{Fe}) for the proposed model-based TRM (i.e., 3.6/12.31/27.36/46.81/71.21 W, respectively) and the conventional model-based LM

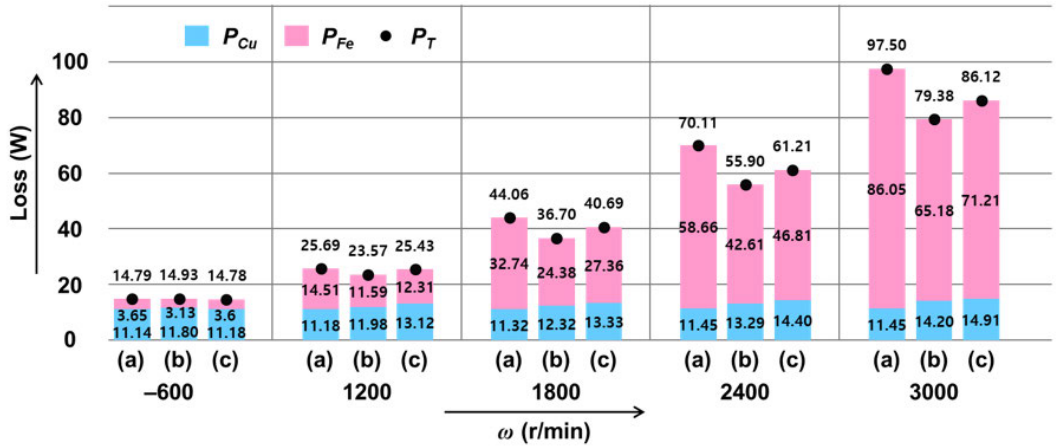

FIGURE 9. Copper loss (P_{Cu}), iron loss (P_{Fe}), and electrical losses (P_T) under *Case 1*. (a) Conventional model-based MTPA. (b) Conventional model-based LM. (c) Proposed model-based TRM.

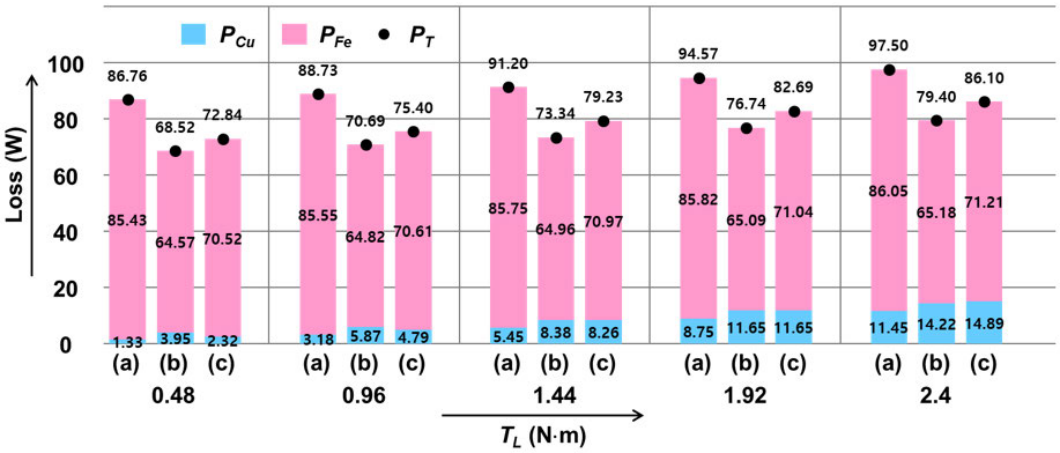

FIGURE 10. Copper loss (P_{Cu}), iron loss (P_{Fe}), and electrical losses (P_T) under *Case 2*. (a) Conventional model-based MTPA. (b) Conventional model-based LM. (c) Proposed model-based TRM.

(i.e., 3.13/11.59/24.38/42.61/65.18 W, respectively) are lower than that of the conventional MTPA (i.e., 3.65/14.51/32.74/58.66/86.05 W, respectively). At each speed change point, it can be observed from Fig. 9 that the P_T of the proposed model-based TRM (i.e., 14.78/25.43/40.69/61.21/86.12 W, respectively) is less than the P_T of the conventional model-based MTPA (i.e., 14.79/25.69/44.06/70.11/97.5 W, respectively).

Fig. 10 shows the values of the P_T in the three control methods under *Case 2*. Unlike the lower P_{Cu} (i.e., 1.33/3.18/5.45/8.75/11.45 W, respectively) of the conventional model-based MTPA during the load torque (T_L) change (i.e., T_L: 0.48 → 0.96 → 1.44 → 1.92 → 2.4 N · m) under ω_r set at 3000 r/min, the conventional model-based LM has the lower values of the P_{Fe} (i.e., 64.57/64.82/64.96/65.09/65.18 W, respectively) and P_T (i.e., 68.52/70.69/73.34/76.74/79.4 W, respectively). Moreover, the conventional model-based LM is similar to the proposed model-based TRM in terms of the P_{Fe} (i.e., 70.52/70.61/70.97/71.04/71.21 W, respectively) and P_T (i.e., 72.84/75.4/79.23/82.69/86.1 W, respectively) because they seek out the optimal values of the i_{ds} for minimizing the electrical losses (P_T) [19]–[21].

Table 2 summarizes the comparative torque ripples (TRs), stator currents (i_{ds} and i_{qs}), and iron loss (P_{Fe}) of the three control methods under *Case 1* (i.e., ω_r: −600 → 1200 → 1800 → 2400 → 3000 r/min under T_L set at 2.4 N · m). Based on the evaluation of the effectiveness for the torque ripple minimization (13), it can be observed that the proposed model-based TRM attains the smaller TRs (i.e., TRs: 0.71 to 0.79 N · m) with smaller torque ripple factor (TRF) (i.e., TRF: 29.1 to 32.38%) than the conventional model-based MTPA (i.e., TRs: 1.02 to 1.06 N·m and TRF: 41.8 to 44.16%) and the conventional model-based LM (i.e., TRs: 1.14 to 1.19 N · m and TRF: 46.72 to 48.77%). Under the fixed load torque (2.4 N · m), the i_{qs} values in the three different control methods are maintained at 5.1 A. On the other hand, the i_{ds} is almost zero for the conventional MTPA and increases for the

TABLE 2. Comparative torque ripples, stator currents, and iron loss of the three control methods under *Case 1*.

Control Method	Speed (r/min)	Power (W)	TRs (N·m)	TRF (%)	i_{ds} (A)	i_{qs} (A)	P_{Fe} (W)
①	–600	150.80	1.06	44.16	0	5.09	3.65
	1200	301.59	1.02	41.80	0	5.1	14.51
	1800	452.39	1.03	42.21	0	5.13	32.74
	2400	603.19	1.03	42.21	0	5.16	58.66
	3000	753.98	1.02	41.80	0	5.16	86.05
②	–600	150.80	1.17	48.75	−1.20	5.1	3.13
	1200	301.59	1.18	48.36	−1.32	5.11	11.59
	1800	452.39	1.16	47.54	−1.56	5.12	24.38
	2400	603.19	1.19	48.77	−2.07	5.16	42.61
	3000	753.98	1.14	46.72	−2.51	5.17	65.18
③	–600	150.80	0.77	32.08	−0.3	5.1	3.6
	1200	301.59	0.76	31.15	−2.1	5.11	12.31
	1800	452.39	0.77	31.56	−2.19	5.12	27.36
	2400	603.19	0.79	32.38	−2.62	5.16	46.81
	3000	753.98	0.71	29.10	−2.82	5.17	71.21

Note that the "①", "②", and "③" represent the conventional model-based MTPA, the conventional model-based LM, and the proposed model-based TRM, respectively.

conventional LM (from –1.20 to –2.51 A) and the proposed TRM (from 0 to –2.82 A). As the speed increases from –600 to 1200 r/min and 1200 to 3000 r/min, the i_{ds} of the proposed TRM suddenly increases from –0.3 to –2.1 A and –2.1 to –2.82 A, respectively. In Fig. 9 and Table 2, the conventional LM and the proposed TRM have a significantly lower P_{Fe} than the P_{Cu}, which ultimately leads to the lower electrical losses (P_T) compared to the conventional MTPA. Meanwhile, the conventional LM has lower P_T, but it has higher TRs. Thus, in order to achieve the lower TRs and lower P_T, the proposed model-based TRM is superior to the conventional model-based MTPA and the conventional model-based LM.

Table 3 encapsulates the comparative torque ripples (TRs), stator currents (i_{ds} and i_{qs}), and iron loss (P_{Fe}) under *Case 2*. It can be seen that the smaller TRs with smaller TRF are observed in the proposed model-based TRM (i.e., TRs: 0.63 to 0.74 N · m and TRF: 25.82 to 30.33%) than the conventional model-based MTPA (i.e., TRs: 0.92 to 0.98 N·m and TRF: 37.7 to 40.16%) and the conventional model-based LM (i.e., TRs: 1.08 to 1.1 N · m and TRF: 44.26 to 45.08%). With the increase in the load torque, the values of the i_{qs} in the three different control methods also rise. Unlike the conventional MTPA, the values of the i_{ds} in the conventional LM and the proposed TRM are more negative, which results in the larger P_{Cu}. However, the smaller electrical losses (P_T) of the conventional LM and the proposed TRM are observed than that of the conventional MTPA due to a significant reduction in the iron loss (P_{Fe}). As seen in Fig. 10 and Table 3, the reduction capability of the P_T in the conventional LM and the proposed TRM is almost the same, but the TRs in the conventional are higher. Thus, by considering the tradeoff between the TR and P_T, the proposed model-based

TABLE 3. Comparative torque ripples, stator currents, and iron loss of the three control methods under *Case 2*.

Control Method	Load Torque (N·m)	Power (W)	TRs (N·m)	TRF (%)	i_{ds} (A)	i_{qs} (A)	P_{Fe} (W)
①	0.48	150.80	0.94	38.52	0	1.76	85.43
	0.96	301.59	0.92	37.70	0	2.72	85.55
	1.44	452.39	0.98	40.16	0	3.56	85.75
	1.92	603.19	0.93	38.11	0	4.51	85.82
	2.4	753.98	0.96	39.34	0	5.16	86.05
②	0.48	150.80	1.10	45.08	−2.48	1.74	64.57
	0.96	301.59	1.08	44.26	−2.51	2.71	64.82
	1.44	452.39	1.1	45.08	−2.54	3.61	64.96
	1.92	603.19	1.09	44.67	−2.49	4.57	65.09
	2.4	753.98	1.08	44.26	−2.52	5.17	65.18
③	0.48	150.80	0.72	29.51	−1.56	1.72	70.52
	0.96	301.59	0.74	30.33	−2.03	2.65	70.61
	1.44	452.39	0.69	28.28	−2.53	3.58	70.97
	1.92	603.19	0.71	29.10	−2.75	4.42	71.04
	2.4	753.98	0.63	25.82	−2.81	5.17	71.21

Note that the "①", "②", and "③" represent the conventional model-based MTPA, the conventional model-based LM, and the proposed model-based TRM, respectively.

TRM has the improved performance over the conventional model-based MTPA and conventional model-based LM.

IV. CONCLUSION

This paper proposes an enhanced TRM technique using model-based LM control for VSI-fed SPMSM drives with a core loss resistance. In this paper, the proposed control design is targeted to decrease the torque ripples and improve the efficiency. Then the proposed TRM is validated by the comparative experimental studies on a prototype SPMSM drive with a real-time TI TMS320F28335 DSP. From the comparative experimental results, it is observed that the torque ripples of the proposed model-based TRM are significantly reduced in comparison with the conventional model-based MTPA and conventional model-based LM by selecting the appropriate value of the demagnetizing reference current (i_{odr}). Even if the d-axis stator current increases the copper loss (P_{Cu}) of the SPMSM, the proposed TRM minimizes the electrical losses (P_T) similar to the conventional model-based LM by achieving the smaller iron loss (P_{Fe}) than the conventional model-based MTPA.

REFERENCES

[1] G. Pei, L. Li, X. Gao, J. Liu, and R. Kennel, "Predictive current trajectory control for PMSM at voltage limit," *IEEE Access*, vol. 8, pp. 1670–1679, 2020.
[2] C. Zhu, Z. Zeng, and R. Zhao, "Comprehensive analysis and reduction of torque ripples in three-phase four-switch inverter-fed PMSM drives using space vector pulse-width modulation," *IEEE Trans. Power Electron.*, vol. 32, no. 7, pp. 5411–5424, Jul. 2017.
[3] V. Q. Leu, H.-H. Choi, and J.-W. Jung, "LMI-based sliding mode speed tracking control design for surface-mounted permanent magnet synchronous motors," *J. Electr. Eng. Technol.*, vol. 7, no. 4, pp. 513–523, Jul. 2012.

[4] T. U. Jung and C. S. Park, "A torque compensation method considering temperature variation of SPMSM," *J. Electr. Eng. Technol.*, vol. 13, no. 1, pp. 160–167, Jan. 2018.
[5] G. Feng, C. Lai, and N. C. Kar, "Practical testing solutions to optimal stator harmonic current design for PMSM torque ripple minimization using speed harmonics," *IEEE Trans. Power Electron.*, vol. 33, no. 6, pp. 5181–5191, Jun. 2018.
[6] W. Wang, H. Ma, X. Qiu, and J. Yang, "A calculation method for the on-load cogging torque of permanent magnet synchronous machine," *IEEE Access*, vol. 7, pp. 106316–106326, 2019.
[7] M. Liu, K. W. Chan, J. Hu, W. Xu, and J. Rodriguez, "Model predictive direct speed control with torque oscillation reduction for PMSM drives," *IEEE Trans. Ind. Informat.*, vol. 15, no. 9, pp. 4944–4956, Sep. 2019.
[8] Y. Cho, K.-B. Lee, J.-H. Song, and Y. I. Lee, "Torque-ripple minimization and fast dynamic scheme for torque predictive control of permanent-magnet synchronous motors," *IEEE Trans. Power Electron.*, vol. 30, no. 4, pp. 2182–2190, Apr. 2015.
[9] M. H. Vafaie, B. M. Dehkordi, P. Moallem, and A. Kiyoumarsi, "Improving the steady-state and transient-state performances of PMSM through an advanced deadbeat direct torque and flux control system," *IEEE Trans. Power Electron.*, vol. 32, no. 4, pp. 2964–2975, Apr. 2017.
[10] H. M. Flieh, R. D. Lorenz, E. Totoki, S. Yamaguchi, and Y. Nakamura, "Dynamic loss minimizing control of a permanent magnet servomotor operating even at the voltage limit when using deadbeat-direct torque and flux control," *IEEE Trans. Ind. Appl.*, vol. 55, no. 3, pp. 2710–2720, May 2019.
[11] J. Liu, H. Li, and Y. Deng, "Torque ripple minimization of PMSM based on robust ILC via adaptive sliding mode control," *IEEE Trans. Power Electron.*, vol. 33, no. 4, pp. 3655–3671, Apr. 2018.
[12] X. Zhang, "Discussion on 'torque ripple minimization of PMSM based on robust ILC via adaptive sliding mode control,'" *IEEE Access*, vol. 7, pp. 94899–94906, 2019.
[13] P. Mattavelli, L. Tubiana, and M. Zigliotto, "Torque-ripple reduction in PM synchronous motor drives using repetitive current control," *IEEE Trans. Power Electron.*, vol. 20, no. 6, pp. 1423–1431, Nov. 2005.
[14] S. Li, M. Zhou, and X. Yu, "Design and implementation of terminal sliding mode control method for PMSM speed regulation system," *IEEE Trans. Ind. Informat.*, vol. 9, no. 4, pp. 1879–1891, Nov. 2013.
[15] X. Zhang, L. Sun, K. Zhao, and L. Sun, "Nonlinear speed control for PMSM system using sliding-mode control and disturbance compensation techniques," *IEEE Trans. Power Electron.*, vol. 28, no. 3, pp. 1358–1365, Mar. 2013.
[16] Q. Liu and K. Hameyer, "Torque ripple minimization for direct torque control of PMSM with modified FCSMPC," *IEEE Trans. Ind. Appl.*, vol. 52, no. 6, pp. 4855–4864, Nov. 2016.
[17] R. Ni, D. Xu, G. Wang, L. Ding, G. Zhang, and L. Qu, "Maximum efficiency per ampere control of permanent-magnet synchronous machines," *IEEE Trans. Ind. Electron.*, vol. 62, no. 4, pp. 2135–2143, Apr. 2015.
[18] S. Morimoto, Y. Tong, Y. Takeda, and T. Hirasa, "Loss minimization control of permanent magnet synchronous motor drives," *IEEE Trans. Ind. Electron.*, vol. 41, no. 5, pp. 511–517, Oct. 1994.
[19] J. Lee, K. Nam, S. Choi, and S. Kwon, "Loss-minimizing control of PMSM with the use of polynomial approximations," *IEEE Trans. Power Electron.*, vol. 24, no. 4, pp. 1071–1082, Apr. 2009.
[20] S. M. Tripathi and C. Dutta, "Enhanced efficiency in vector control of a surface-mounted PMSM drive," *J. Franklin Inst.*, vol. 355, no. 5, pp. 2392–2423, Mar. 2018.
[21] H. Pairo and A. Shoulaie, "Effective and simplified method in maximum efficiency control of interior permanent magnet synchronous motors," *IET Electric Power Appl.*, vol. 11, no. 3, pp. 447–459, Mar. 2017.
[22] H. Ge, Y. Miao, B. Bilgin, B. Nahid-Mobarakeh, and A. Emadi, "Speed range extended maximum torque per ampere control for PM drives considering inverter and motor nonlinearities," *IEEE Trans. Power Electron.*, vol. 32, no. 9, pp. 7151–7159, Sep. 2017.
[23] H. Liu, Z. Q. Zhu, E. Mohamed, Y. Fu, and X. Qi, "Flux-weakening control of nonsalient pole PMSM having large winding inductance, accounting for resistive voltage drop and inverter nonlinearities," *IEEE Trans. Power Electron.*, vol. 27, no. 2, pp. 942–952, Feb. 2012.
[24] W. Qian, S. K. Panda, and J.-X. Xu, "Torque ripple minimization in PM synchronous motors using iterative learning control," *IEEE Trans. Power Electron.*, vol. 19, no. 2, pp. 272–279, Mar. 2004.
[25] S. H. Kim, *Electric Motor Control: DC, AC, and BLDC Motors*. Amsterdam, The Netherlands: Elsevier, 2017.

JINUK KIM received the B.S. degree in electronic engineering from Dongguk University, Seoul, South Korea, in 2014, where he is currently pursuing the Ph.D. degree with the Division of Electronics and Electrical Engineering.

His research interests include the field of electric machine drives based on microprocessor, control of distributed generation systems using renewable energy sources, and power conversion systems and drives for electric vehicles.

SANG-WOOK RYU received the B.S. degree in electronics and electrical engineering from Dongguk University, Seoul, South Korea, in 2018, where he is currently pursuing the Ph.D. degree.

His research interests include DSP-based electric machine drives, electric vehicles, smart grid-enabling technologies, and integration of renewable energy sources in modern power systems.

MUHAMMAD SAAD RAFAQ received the B.S. degree in electrical engineering from the University of Engineering and Technology, Taxila, Pakistan, in 2011, and the Ph.D. degree from the Division of Electronics and Electrical Engineering, Dongguk University, Seoul, South Korea, in 2019.

From 2012 to 2013, he was a Laboratory Engineer with the University of Gujrat, Gujrat, Pakistan. His research interests include distributed generation systems, control of power converters, parameter identification, electric vehicles, and DSP-based electric machine drives.

HAN HO CHOI (Member, IEEE) received the B.S. degree in control and instrumentation engineering from Seoul National University, Seoul, South Korea, in 1988, and the M.S. and Ph.D. degrees in electrical engineering from the Korea Advanced Institute of Science and Technology, Daejeon, South Korea, in 1990 and 1994, respectively.

He is currently with the Division of Electronics and Electrical Engineering, Dongguk University, Seoul. His research interests include control theory and its applications to real-world problems.

JIN-WOO JUNG (Member, IEEE) received the B.S. and M.S. degrees in electrical engineering from Hanyang University, Seoul, South Korea, in 1991 and 1997, respectively, and the Ph.D. degree in electrical and computer engineering from The Ohio State University, Columbus, OH, USA, in 2005.

From 1997 to 2000, he was with the Home Appliance Research Laboratory, LG Electronics Company, Limited, Seoul. From 2005 to 2008, he was a Senior Engineer with the Research and Development Center, and with the PDP Development Team, Samsung SDI Company, Limited, South Korea. Since 2008, he has been a Professor with the Division of Electronics and Electrical Engineering, Dongguk University, Seoul. His research interests include DSP-based electric machine drives, distributed generation systems using renewable energy sources, and power conversion systems and drives for electric vehicles.